

Adsorption of rare-gas atoms on Cu(111) and Pb(111) surfaces by van der Waals-corrected Density Functional Theory

Pier Luigi Silvestrelli, Alberto Ambrosetti, Sonja Grubisić,* and Francesco Ancilotto
*Dipartimento di Fisica, Università di Padova, via Marzolo 8, I-35131,
Padova, Italy, and DEMOCRITOS National Simulation Center, Trieste, Italy*

The DFT/vdW-WF method, recently developed to include the Van der Waals interactions in Density Functional Theory (DFT) using the Maximally Localized Wannier functions, is applied to the study of the adsorption of rare-gas atoms (Ne, Ar, Kr, and Xe) on the Cu(111) and Pb(111) surfaces, at three high-symmetry sites. We evaluate the equilibrium binding energies and distances, and the induced work-function changes and dipole moments. We find that, for Ne, Ar, and Kr on the Cu(111) surface the different adsorption configurations are characterized by very similar binding energies, while the favored adsorption site for Xe on Cu(111) is on top of a Cu atom, in agreement with previous theoretical calculations and experimental findings, and in common with other close-packed metal surfaces. Instead, the favored site is always the hollow one on the Pb(111) surface, which therefore represents an interesting system where the investigation of high-coordination sites is possible. Moreover, the Pb(111) substrate is subject, upon rare-gas adsorption, to a significantly smaller change in the work function (and to a correspondingly smaller induced dipole moment) than Cu(111). The role of the chosen reference DFT functional and of different Van der Waals corrections, and their dependence on different rare-gas adatoms, are also discussed.

PACS numbers:

I. INTRODUCTION

Understanding adsorption processes on solid surfaces is essential to design and optimize countless material applications, and to interpret, for instance, scattering experiments and atomic-force microscopy. In particular, the adsorption of rare-gas (RG) atoms on metal surfaces is prototypical² for physisorption processes. Basically, the weak binding of physisorbed closed electron-shell atoms, such as RG atoms, is due to an equilibrium between attractive, long-range van der Waals (vdW) interactions and short-range Pauli repulsion acting between the electronic charge densities of the substrate and the adatoms.³

Up to now RG adsorption on many close-packed metal surfaces, such as Ag(111), Al(111), Cu(111), Pd(111), Pt(111),... have been extensively studied both experimentally⁴⁻⁷ and theoretically,⁷⁻¹⁴ while, to our knowledge, Pb has not, but for the experimental measurements of Ferralis *et al.*¹⁵ and, very recently, the theoretical investigation of Zhang *et al.*,¹⁶ who studied the tribological properties of Ne and Kr on the Pb(111) surface. The Pb surface is important for practical applications: for instance, there is considerable interest in the frictional (tribological) properties of gases on Pb at low temperatures; in particular, Pb is used¹⁵⁻¹⁷ as a material for the electrodes and as adsorption surfaces in nanofriction experiments because it is easy to grow a very uniform film already at room temperature and to remove the surface contaminants deposited over time on the electrodes, thanks to its large diffusion coefficient. The Pb(111) surface also exhibits interesting and unusual properties: for instance, one striking finding is the drastic difference between the sliding friction of Ne and Kr mono- or multilayers.^{16,17}

In principle, due to the non-directional character of

the vdW interactions that should be the dominant one in physisorption processes, surface sites that maximize the coordination of the RG adsorbate atom were expected to be the preferred ones, so that it was usually assumed that the adsorbate occupies the maximally coordinated *hollow* site. This assumption was also based on the expectation that the atom in the *hollow* site would be closer to the surface, thus experiencing a more attractive potential; behind this is the notion that the repulsive potential at the surface is proportional to the atomic charge density and the natural assumption is that the charge density is highest at the locations of the atoms, thus making the *top* site energetically unfavored. Calculations where the total adatom-substrate interaction is described by the sum of empirical binary potentials, which are widely used and often give reasonable results for adsorption energies, seem to confirm this expectation since the highly coordinated *hollow* sites naturally emerge as the preferred adsorption sites for the adatoms. However this picture has been questioned by many experimental⁴⁻⁶ and theoretical⁹⁻¹² recent studies which indicate that the actual scenario is more complex: in particular, for Xe and Kr a general tendency is found^{7,9-12} for adsorption on metallic surfaces in the low-coordination *top* sites (this behavior was attributed^{7,18} to the delocalization of charge density that increases the Pauli repulsion effect at the *hollow* sites relative to the *top* site and lifts the potential well upwards both in energy and height); for Ar the situation seems to be less clear:¹⁰ for instance, comparison of theoretical and experimental results⁷ would suggest that the *hollow* sites is still favored for Ar on Ag(111).

The importance of polarization effects to determine the favored adsorption sites was pointed out by Da Silva *et al.*,¹⁰ who studied the interaction of RG adatoms with the Pd(111) surface: in fact, for instance, for Xe the

polarization is larger in the on-top site, i.e. the larger induced dipole moment increases the attractive interaction between Xe and the metal surface. Therefore, the dominant mechanisms appear to be polarization-induced attraction and site-dependent Pauli repulsion. The latter, being weaker for the on-top site, stabilizes on-top adsorption.⁸

In spite of this recent substantial progress, the understanding of the interaction of RGs with metal surfaces is not complete yet.⁷ It is not clear, for instance, whether a system exists where high-coordinated sites are always preferred. Moreover, there have been relatively few studies of adsorption geometries for the smaller RGs, although these are probably better candidates for the observation of high-coordination sites, due to their reduced polarizability with respect to that of Xe or Kr: in fact, the considerable mismatch between the lattice constants of the smaller RGs and that of most metal surfaces cause most commensurate structures to have multiple atoms per unit cell, so that the characterization and interpretation of such systems is quite complex.

Density Functional Theory (DFT) is a well-established computational approach to study the structural and electronic properties of condensed matter systems from first principles, and, in particular, to elucidate complex surface processes such as adsorptions, catalytic reactions, and diffusive motions. Although current density functionals are able to describe quantitatively condensed matter systems at much lower computational cost than other first principles methods, they fail¹⁹ to properly describe dispersion interactions. Dispersion forces originate from correlated charge oscillations in separate fragments of matter and the most important component is represented by the R^{-6} vdW interaction,²⁰ originating from correlated instantaneous dipole fluctuations, which plays a fundamental role in adsorption processes of fragments weakly interacting with a substrate ("physisorbed").

This is clearly the case for the present systems which can be divided into well separated fragments (RG atoms and the metal substrate) with negligible electron-density overlap. The local or semilocal character of the most commonly employed exchange-correlation functionals makes DFT methods unable to correctly predict binding energies and equilibrium distances within both the local density (LDA) and the generalized gradient (GGA) approximations.²¹ As a consequence, the basic results often depend, even at a qualitative level, on the adopted DFT functional: for instance, in their *ab initio* study of the interaction of RG adatoms with the Pd(111) surface, Da Silva *et al.*¹⁰ found that the on-top site preference is obtained by the LDA for all RG adatoms, while the GGA functionals (in the PBE and PW91 schemes) yield the on-top site preference for Xe, Kr, and He adatoms, but the *hollow* site for Ne and Ar. Typically, in many physisorbed systems GGAs give only a shallow and flat adsorption well at large atom-substrate separations, while the LDA binding energy turns out to be not far from the experimental adsorption energy; however, since it is well known

that LDA tends to overestimate the binding in systems with inhomogeneous electron density (and to underestimate the equilibrium distances), the reasonable performances of LDA must be considered as accidental. Therefore, a theoretical approach beyond the DFT-LDA/GGA framework, that is able to properly describe vdW effects is required to provide more quantitative results.¹⁰

In the last few years a variety of practical methods have been proposed to make DFT calculations able to accurately describe vdW effects (for a recent review, see, for instance, ref. 21). We have investigated by such a method the adsorption of RG atoms on the Cu(111) and Pb(111) surfaces. Cu(111) has been chosen because of the many experimental and theoretical data available (especially for Xe-Cu(111)), which can be compared with ours in such a way to validate the present approach; as mentioned above, the less studied Pb(111) surface could be interesting because, given the relatively large Pb lattice constant (and hence nearest-neighbor surface Pb-Pb distance) it represents a good candidate for a system where RG atoms are preferably adsorbed on *hollow* sites (the lattice constant of Pb is 4.95 Å, compared to 4.09 Å for Ag, 4.05 Å for Al, 3.92 Å for Pt, 3.89 Å for Pd, and 3.61 Å for Cu).

II. METHOD

In this study we include vdW effects within a standard DFT approach by using the method proposed in refs. 22–24 (where further details can be found), hereafter referred to as DFT/vdW-WF, by introducing an additional term in the exchange-correlation functional as originally proposed by Andersson *et al.*²⁵ to describe the interactions between separate fragments. This contribution, which effectively accounts for the dispersion forces both in the uniform electron gas and separate atom limits, has the form :

$$E_{vdW} = - \sum_{n,l} f_{nl}(r_{nl}) \frac{C_{6nl}}{r_{nl}^6} \quad (1)$$

with (in a.u.)

$$C_{6nl} = \frac{3}{16\pi^{3/2}} \int_{|\mathbf{r}'| < r'_c} d\mathbf{r}' \int_{|\mathbf{r}| < r_c} d\mathbf{r} \frac{\sqrt{\rho_n(r)\rho_l(r')}}{\sqrt{\rho_n(r) + \sqrt{\rho_l(r')}}}. \quad (2)$$

In the above formulas r_{nl} is the distance between the two separate fragments n and l , and $\rho_n(r)$ is the n -th fragment electronic density. The cutoff r_c is introduced to remove the divergence of the integral, taking into account that, at small momentum values, the interaction is highly damped.²⁵

In our approach all the fragment densities are conveniently rewritten in terms of the Maximally Localized Wannier Functions (MLWFs), $\{w_n(r)\}$, i.e. $\rho_n(r) = w_n^2(r)$. The MLWFs can be obtained from the occupied

Kohn-Sham orbitals, generated by a standard DFT calculation, by means of a unitary transformation which minimizes the functional²⁶

$$\Omega = \sum_n S_n^2 = \sum_n (\langle w_n | r^2 | w_n \rangle - \langle w_n | \mathbf{r} | w_n \rangle^2). \quad (3)$$

The unitary transformation conserves the total density, which is however partitioned into single localized fragments, each of them being characterized by its spread S_n and center of mass position r_n . It is therefore possible to express the vdW correction (see eqs. (1) and (2)) as a sum of single contributions coming from each pair of Wannier functions belonging to different fragments, by approximating the shape of the n -th Wannier function²⁴ with an H-like exponential.

The DFT/vdW-WF method has been already successfully applied to several systems, including small molecules, bulk, and surfaces;^{22–24,27–29} in particular it allowed us to study the interaction of Ar with graphite and of Ar, He, and H₂ with Al surfaces,^{23,24} of water with the Cl- and H-terminated Si(111) surfaces,²⁸ and of RG atoms and water with graphite and graphene.²⁹

We here apply the DFT/vdW-WF method to the case of adsorption of Ne, Ar, Kr, and Xe atoms on the Cu(111) and Pb(111) surfaces. All calculations have been performed with the Quantum-ESPRESSO³⁰ ab initio package (MLWFs have been generated as a post-processing calculation using the WanT package³¹). Similarly to DaSilva *et al.*,¹⁰ we modeled the clean and RG-covered metal surfaces using a periodically-repeated hexagonal supercell, with a $(\sqrt{3} \times \sqrt{3})R30^\circ$ structure and a surface slab made of 15 metal (Cu or Pb) atoms distributed over 5 layers (repeated slabs were separated along the direction orthogonal to the surface by a vacuum region of about 24 Å). The Brillouin Zone has been sampled using a $6 \times 6 \times 1$ k -point mesh. In this model system the RG coverage is 1/3, i.e. one RG adatom for each 3 metal atoms in the topmost surface layer. The $(\sqrt{3} \times \sqrt{3})R30^\circ$ structure has been indeed observed at low temperature by LEED for the case of Xe adsorption on Cu(111) and Pd(111)⁵ (actually, this is the simplest commensurate structure for RG monolayers on close-packed metal surfaces and the only one for which good experimental data exist), and it was adopted in most of the previous ab initio studies^{8–10,12,13,16}. Since the lateral interactions between RG adatoms do not play a critical role in the RG adsorption site preference,⁹ for the sake of simplicity, we have used the same structure also for the other RGs (Ne, Ar, and Kr) and in the case of adsorption on Pb(111) as well.

The Pb or Cu surface atoms were kept frozen (of course after a preliminary relaxation of the outermost layers of the clean metal surfaces) and only the vertical coordinates of the RG atoms, perpendicular to the surface, were optimized, this procedure being justified by the fact that only minor surface atom displacements are observed upon physisorption.^{9,16,32} Moreover, the RG atoms were adsorbed on both sides of the slab: in this way the sur-

face dipole generated by adsorption on the upper surface of the slab is cancelled by the dipole appearing on the lower surface, thus greatly reducing the spurious dipole-dipole interactions between the periodically repeated images (previous DFT-based calculations have shown that these choices are appropriate^{10,14}). Note that, apparently, in their recent study of Ne and Kr on Pb(111), Zhang *et al.*¹⁶ have instead considered adsorption on a single side of the metal slab; the effect of such a choice is non-negligible: in fact, for instance, in the case of Xe on Pb(111), we find that the (absolute value of the) binding energy is reduced by 7 meV (about 4 %) with respect to that obtained when Xe is adsorbed on both sides of the slab. The results of ref. 16 are thus likely affected by the artificial dipole-dipole interactions discussed above.

We have carried out calculations for various separations of the RG atoms adsorbed on high-symmetry sites, namely *hollow* (on the center of the triangle formed by the 3 surface metal atoms contained in the supercell), *top* (on the top of a metal atom), and *bridge* (intermediate between two nearest-neighbor metal atoms). Actually, two kinds of *hollow* sites are present: HCP *hollows*, characterized by having atoms directly beneath them in the next layer of atoms, and FCC *hollows* where this condition does not apply; however the HCP-*hollow* and the FCC-*hollow* sites can be considered equivalent for adsorption because of the small differences in the adsorption properties (for instance, Righi and Ferrario,¹³ using LDA, found a difference of less than 1 meV in the adsorption energy and of 0.01 Å in the equilibrium distance for RGs adsorbed on Cu(111)). For a better accuracy, as done in previous applications on adsorption processes,^{23,24,28,29} we have also included the interactions of the MLWFs of the physisorbed fragments not only with the MLWFs of the underlying surface, within the reference supercell, but also with a sufficient number of periodically-repeated surface MLWFs (in any case, given the R^{-6} decay of the vdW interactions, the convergence with the number of repeated images is rapidly achieved). Electron-ion interactions were described using norm-conserving pseudopotentials: in the case of Pb and Cu we have explicitly included 14 and 11 valence electrons per atom, respectively (those coming from the $5d^{10}$, $6s^2$, $6p^2$ atomic orbitals for Pb, and $3d^{10}$, $4s^1$ for Cu). As a reference DFT functional we chose PW91³³ because it is widely used in ab initio DFT calculations of solids and surfaces and, in particular, was adopted in some previous simulations¹² of Xe interacting with the Cu(111) surface, which facilitates comparison with the results of the present calculations (note that typically PW91 gives similar results to that obtained by PBE,³⁴ which represents another popular GGA functional). Using the PW91 functional in test calculations with bulk Pb and Cu, for the equilibrium properties the agreement with experimental estimates is comparable to that found in previous DFT calculations.^{9,12,16}

By generating the MLWFs for the Cu(111) and Pb(111) substrates, we observe a clear quantitative separation between the spreads of the MLWFs describing

d -like orbitals and those of the (much more delocalized) MLWFs describing the s - and p -like orbitals; moreover, given the high valence-electron density, screening effects are certainly relevant in these metal surfaces. Therefore, at variance with previous calculations,^{23,24,28,29} we have applied the DFT/vdW-WF correction by explicitly considering only the more localized MLWFs corresponding to the d -like orbitals, while the s - and p -like electrons are supposed to give a screening-effect³⁵ contribution, which is taken into account by multiplying the vdW correction (the C_6 coefficients) by a simple Thomas-Fermi factor: $f_{TF} = e^{-2(z-z_s)/r_{TF}}$ where r_{TF} is the Thomas-Fermi screening length relative to the electronic density of a uniform electron gas ("jellium model") equal to the average density of the s - and p -like electrons of the present systems, z_s is the average vertical position of the topmost Cu or Pb atoms, and z is the vertical position, measured with respect to z_s , of the adatom. In practice it turns out that only the topmost metal layer gives a relevant contribution, while the effects of the other ones is dramatically reduced by the exponential factor, in line with the common expectation about screening effects in metal surfaces.³⁵ This observation can be exploited to considerably reduce the computational cost of the vdW correction since only the topmost MLWFs must be really taken into account.

III. RESULTS AND DISCUSSION

In Tables I-VI results are reported for all the systems under consideration, for adsorption on *hollow*, *top*, and *bridge* sites. The *binding energy*, E_b , is defined as

$$E_b = 1/2(E_{tot} - (E_s + 2E_{RG})) \quad (4)$$

where $E_{s,RG}$ represent the energies of the isolated fragments (the substrate and the RG atoms) and E_{tot} is the energy of the interacting system, including the vdW-correction term (the factors 2 and 1/2 are due to the adsorption of RG atoms on both sides of the slab).

One should point out that the experimentally measured *adsorption energy*, E_a , includes not only the interaction of RG atoms with the substrate but also lateral, vdW, RG-RG interactions;¹⁴ however in most of previous calculations the mostly attractive lateral interaction contribution was not considered. As pointed out, for instance, by Lee *et al.*,³⁶ who studied n -butane on transition-metal surfaces (another typical weak physisorption system where vdW interaction is the only attractive force between the nonpolar molecule and the substrate) lateral adatom-adatom interaction energies can be as large as 25% of the total adsorption energy at full coverage. E_a is here defined as:

$$E_a = E_b + (E_l - E_f),$$

where E_l is the total energy (per atom) of the 2D RG lattice (that is as in the adsorption configurations but without the substrate) and E_f is the energy of an isolated RG atom. Clearly the quantity in parenthesis in

the above formula represents the lateral adatom-adatom interaction energy (per atom). Note that, in their DFT study of Ne and Kr on Pb(111), Zhang *et al.*¹⁶ seem instead to identify E_a with E_b .

E_b has been evaluated for several adsorbate-substrate distances; then the equilibrium distances and the corresponding binding energies have been obtained by fitting the calculated points with the function: $Ae^{-Bz} - C_3/(z - z_0)^3$, A , B , C_3 , and z_0 being adjustable parameters (as illustrated for the Xe-Cu(111) and Xe-Pb(111) cases in Figs. 1 and 2). Typical uncertainties in the fit are of the order of 0.05 Å for the distances and a few meV for the minimum binding energies. Our results are compared to available theoretical and experimental estimates and to corresponding data obtained using a pure PW91 functional, the simple LDA functional, and the "seamless" vdW-DF method of Langreth *et al.*³⁷ (note that the vdW-DF method has been also used in the recent DFT study of Zhang *et al.*¹⁶). As can be seen in Figs. 1 and 2, and in Tables I and II, the effect of the vdW correction computed by DFT/vdW-WF is a much stronger bonding than with a pure PW91 scheme, with the formation of a clear minimum in the binding energy curve at a shorter equilibrium distance. In spite of the clear shortcomings of the pure PW91 scheme, in general the preferred adsorption site seems to be correctly determined by the latter, although the differences between the binding energies of the different adsorption sites are very small.

We have also computed E_a (assuming a full monolayer coverage of RGs) in the case of Xe on Cu(111), where a RG overlayer in the $(\sqrt{3} \times \sqrt{3})R30^\circ$ structure is experimentally found⁵ and in the case of Xe on Pb(111), where the formation of a commensurate Xe monolayer was also observed.¹⁵ As can be seen in Table III, all the methods, but pure PW91, correctly predict a smaller E_a on Pb(111) than on Cu(111), although the quantitative results considerably depend on the adopted scheme: in fact, pure PW91 clearly underestimates E_a , DFT/vdW-WF and vdW-DF give comparable results, while LDA is close to DFT/vdW-WF and vdW-DF for Xe on Cu(111) but underestimates for Xe on Pb(111): this can be explained by the fact that LDA is not able to describe properly the lateral interactions of Xe adatoms which are further from each other on Pb(111) than on Cu(111).

Concerning the adsorption on the Cu(111) surface (see Table I), all the methods used predict that the *top* configuration is energetically favored in the case of Xe, while for Ne, Ar, and Kr the differences among the binding energies of the different adsorption configurations are quite small (using vdW-DF the same is true also for Xe); since these differences are probably comparable to the expected accuracy of the calculations, a precise assignment of the favored adsorption site is not possible. In contrast, the *hollow* configuration is instead clearly favored by all the methods (see Table II) in the case of the adsorption on Pb(111) of all the considered RG atoms (actually, with DFT/vdW-WF, for Ar on Pb(111) the

bridge site appears to be lower in energy: however, given the small difference with the energy of the *hollow* site, this result should not be overemphasized). Our results for Pb(111) are in qualitative agreement with those of Zhang *et al.*¹⁶ who predict that Ne and Kr indeed prefer high-coordination *hollow* sites. Note that the energy difference between the *hollow* and *top* sites increases by subsequently considering the PW91, vdW-DF, DFT/vdW-WF, and LDA methods (see also Da Silva *et al.*⁹).

Interestingly, in the case where several experimental reference values are available, namely Xe on Cu(111), our DFT/vdW-WF method performs better (considering both the binding and adsorption energy, and the equilibrium distance, see Tables I, III, and IV) than all the other schemes: in fact LDA gives reasonable binding energies but underestimates the equilibrium distances, while vdW-DF underestimates the binding energies and overestimates the equilibrium distances, in line with the behavior reported for systems including a metallic surface.³⁸ Also note that, at a variance with the experimental findings, the vdW-DF method predicts that the *top* site (see Table I) is only marginally favored (and the distance only marginally different) than the *hollow* ones; in general, for all the RG atoms on Cu(111) vdW-DF gives almost identical binding energies for the *top* and *hollow* adsorption sites. In the case of RGs on Pb(111) the *hollow* structure is favored also by vdW-DF, although the difference in the binding energy with respect to the *top* site is smaller than with the present DFT/vdW-WF scheme (the difference was instead larger, see the last column of Table II, in the study of Zhang *et al.*¹⁶, who used vdW-DF but with a reference DFT functional differing from ours by the exchange term). In the case of Ar on Cu(111) and on Pb(111), we observe that our computed binding energies compare favorably with the estimates obtained, using a simple Lennard-Jones potential, by Cheng *et al.*,³⁹ who predicted a binding energy between 70 and 85 meV for Ar on noble metals.

As expected, we find that, both for adsorption on Cu(111) and Pb(111), the binding energy increases by going from Ne to Xe, in line with the increasing polarizability of this atom sequence. In particular, for several close-packed transition-metal surfaces the binding energy of Xe is found¹⁰ to be about 2 to 3 times larger than that of Kr, and Ar, respectively, a behavior which is well reproduced by our DF/vdW-WF method (the factors are 1.5 and 3, and 1.6 and 2.5, for adsorption on Cu(111) and on Pb(111), respectively). This general behavior is also in line with the results of Zhang *et al.*¹⁶

Our energetic results are not far from the "best estimate" reported by Vidali *et al.*³ for Xe on Cu(111), i.e. a binding energy of -183 ± 10 meV at a distance of $3.60 \pm 0.08 \text{ \AA}$ (these values represent averages over different theoretical/experimental estimates). In their tables Vidali *et al.*³ also report for Ar on Cu(111) a binding energy of -85 meV at a distance of 3.53 \AA and for Kr on Cu(111) a binding energy of -119 meV, in fair agreement with our results. Lazic *et al.*¹² studied the adsorption of Xe on

Cu(111) by a DFT approach where vdW corrections were included using the method of Andersson *et al.*,²⁵ using PW91 and PBE as reference DFT functionals (see the last column in Tables I and IV). As can be seen, our results are much closer to the experimental estimate than those of Lazic *et al.*,¹² which tend to overestimate the binding energy and underestimate the equilibrium distance. The Xe-adsorbed Cu(111) surface has been also recently investigated by Sun and Yamauchi¹⁴ using DFT with semiempirical vdW corrections: they found reasonable equilibrium distances, however the computed binding energy was very overestimated (it was even larger than that obtained by LDA) and the favored adsorption site was incorrectly predicted to be the *hollow* site, probably due to the use of semiempirical pair potentials which favor close-packed structures and high coordinated sites (see discussion above).

From Tables I, III, and IV, one can also see that the binding energies are reasonably reproduced by the LDA scheme for RGs on Cu(111), a behavior common to several physisorption systems. However, as already outlined above, this agreement should be considered accidental: the well-known LDA overbinding, due to the overestimate of the long-range part of the exchange contribution, somehow mimics the missing vdW interactions; the equilibrium distances predicted by LDA are clearly underestimated since LDA cannot reproduce the R^{-6} behavior in the interaction potential. For RGs on Pb(111), the LDA binding energies are instead underestimated as a consequence (as discussed above) of the larger equilibrium distances than for RGs on Cu(111).

As already found elsewhere,^{9,10} for all the used schemes, the binding energies correlate with the RG-metal distance: in fact, for a given RG, the configurations having the strongest binding are characterized by the shortest RG-substrate distance. Moreover, all the methods predict that Ar and Xe adatoms get closer to the Cu(111) surface when adsorbed on *top* site, as found in some previous studies.^{9,10,13} Remarkably, this behavior cannot be reproduced^{7,10} using a hard-sphere model, indicating that there is a significant interaction between the Ar and Xe atoms and the Cu(111) surface so that a simple stacking (hard-sphere) model of weakly or noninteracting spheres is not valid (for comparison, in Tables IV and V we also list the sums of the RG atoms and metal atom vdW literature radii). Instead, for adsorption on Pb(111), the adatoms in the *hollow* site are closer to the surface than in the *top* one, in line with the usual behavior. These results can be easily elucidated by analyzing the parameters of the adopted fitting function (see above), $A e^{-Bz} - C_3/(z - z_0)^3$: we find that, as a general rule, at the equilibrium distance, the repulsive potential term is weaker on the favored adsorption site (for instance the *top* site for Xe on Cu(111) and the *hollow* one for Xe on Pb(111)), in agreement with the results of Da Silva *et al.*⁹

Ferralis *et al.*¹⁵ studied the structural and thermal properties of Xe on the Pb(111) surface by LEED. They

observed the formation of a Xe monolayer with an incommensurate hexagonal structure with a lattice parameter similar to that found in bulk Xe (4.33 Å); this structure is aligned with the substrate lattice but has a larger unit cell, similarly to the case of Xe on Ag(111), which is also an aligned incommensurate monolayer. They also found that the heat of adsorption for the first Xe layer is -191 ± 10 meV with an, overlayer-substrate spacing of 3.95 ± 0.10 Å. Looking at Table III we found that our computed E_a (-205.5 meV for the *hollow* adsorption site) is close to the experimental value and in better agreement than with the other methods, although our model structure is not exactly the same observed experimentally; moreover, also the Xe-Pb(111) distance (3.93 Å) is in excellent agreement (see Table V) with that estimated by Ferralis *et al.*,¹⁵ which gives further support to the reliability of our DF/vdW-WF method. As expected, it has been found¹⁵ that a hard-sphere model is unable to give a good description of adsorption of Xe on Pb(111). For Xe-Pb(111) the heat of adsorption is lower than for Xe on any surface measured so far,¹⁵ with the possible exception of Al(110) and for alkali metals; a low heat of adsorption is not particularly surprising since the Pb atoms are much larger than most other metals (the vdW radius of Pb is 2.02 Å, compared to 1.72 Å for Ag, 1.72 Å for Pt, 1.63 Å for Pd, and 1.40 Å for Cu), implying that the repulsive Xe-Pb interaction prevents the Xe from approaching the deeper part of the attractive holding potential. It must be noted that Ferralis *et al.*¹⁵ were unable to determine the preferred adsorption site, the lack of satellite intensities in the LEED patterns indicating that the overlayer is quite uniform and the corrugation is small.

An important quantity which often provides revealing details of the bonding mechanism in adsorption processes is represented by the electron density difference, $\Delta n(\mathbf{r}) = n_{RG/s}(\mathbf{r}) - n_s(\mathbf{r}) - n_{RG}(\mathbf{r})$, obtained from the electron density (at the equilibrium geometry) of the RG on the substrate, of the clean substrate, and the isolated RG monolayer, respectively. Our approach in this respect is not fully self-consistent because we use the electron density obtained at a pure PW91 level, that is without vdW corrections, however, the effects due to the lack of self-consistency are expected to be negligible because the rather weak and diffuse vdW interactions should not substantially change the electronic charge distribution.⁴⁰ Plots of $\Delta n(\mathbf{r})$ for Xe on Cu(111) and Xe on Pb(111), both in the *hollow* and *top* site (see Figs. 3 and 4), show that, in agreement with what found previously¹⁰ for RGs on Pd(111), the electron density redistribution is stronger on the Cu atoms for the Xe on the *top* site than for the *hollow*; both sites exhibit a significant depletion of electron density centered about the Xe atom together with a slight density accumulation close to the center of the Xe atom, this effect being attributed¹⁰ to orthogonalization of Xe states to the states of the substrate atoms. Moreover, for Xe in the on-top site, there is a significant electron density accumulation between the Xe atom and

the topmost surface layer. Interestingly, there is a clear tendency of Xe to induce a much larger charge delocalization on the Cu(111) surface than on Pb(111), in line with the delocalization mechanism invoked^{7,18} to explain the preference for the *top* adsorption site on Cu(111).

Since polarization effects are assumed to play a key role in determining the favored adsorption sites,^{10,13} we have also computed the change of the work function, ΔW , of the Cu(111) and Pb(111) substrate upon adsorption of RG atoms. The work functions have been calculated as the difference between the averaged electrostatic Coulomb potential at the midpoint of the vacuum region of the slab and the Fermi energy:⁴¹ for the clean Cu(111) and Pb(111) surfaces we estimate a work function of 4.85 and 3.86 eV, respectively, in excellent agreement with the reference values, that are in the range from 4.90 to 5.01 eV⁴² for Cu(111), and 3.83 eV for Pb(111).⁴³ ΔW can be related to the dipole moment induced in the substrate by the presence of the RG adatom, $\Delta\mu$, using the Helmholtz equation:⁴⁴

$$\Delta\mu = \frac{1}{12\pi} \frac{A_{(1\times 1)}}{\Theta} \Delta W, \quad (5)$$

where $A_{(1\times 1)}$ is the area of the (1×1) surface unit cell (in Å²) and Θ is the RG coverage; if ΔW is given in eV, then $\Delta\mu$ is in debyes. In our case $\Theta = 1/3$, so that $\Delta\mu = \sqrt{3}a_0^2/16\pi\Delta W$, where a_0 is the Cu or Pb lattice constant. Our computed ΔW and $\Delta\mu$ values are listed in Table VI. In agreement with previous ab initio calculations,^{9,10} we find that the RG adsorption induces a decrease in the work function, thus indicating that the RG atoms behave as adsorbates with an effective positive charge; note that this is consistent with the depletion of the electron density about the Xe atom discussed above, which corresponds to an induced surface dipole moment that points out of the surface. For Xe on Cu(111) our estimated ΔW and $\Delta\mu$ values (see Table VI) agree well with the experimental estimates⁴⁵ of -0.60 eV and -0.24 D, respectively. As can be seen in Table VI, the absolute value of $\Delta\mu$ increases from Ne to Xe, because the corresponding electronic polarizabilities increase, and is larger for the optimal adsorption site, for instance the *top* for Xe on Cu(111) and the *hollow* for Xe on Pb(111). Moreover, it is considerably larger on Cu(111) than on Pb(111) in line with the energetic analysis reported above, that indicated a stronger interaction of RGs with the Cu(111) surface than with Pb(111).

Zhang *et al.*¹⁶ explain the much larger mobility of Ne overlayers on Pb(111), as observed in friction experiments, than of Kr overlayers on the basis of the different activation energies which characterize the lateral motion of Ne and Kr atoms on the Pb(111) surface. The activation energies for a monolayer can be directly calculated from the difference in the binding energy of the adatom between the favored (*hollow*) site and the transition state, which is expected to correspond to the *bridge* site.¹⁶ Considering the differences between the binding energy of

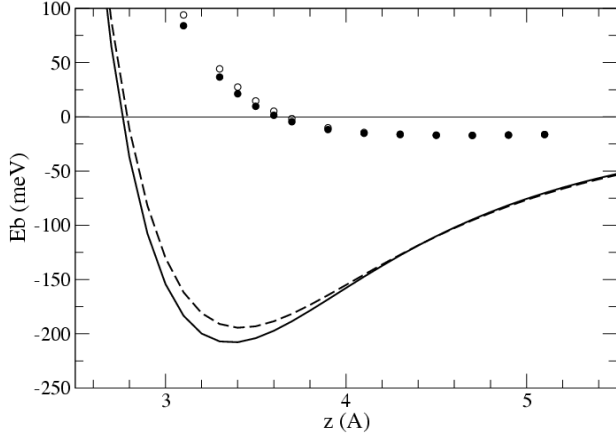


FIG. 1: Binding energy of Xe on Cu(111) in the *top* and *hollow* configuration using pure PW91 (full and empty circles, respectively) and DFT/vdW-WF (solid and dashed line, respectively), as a function of the distance z from the surface.

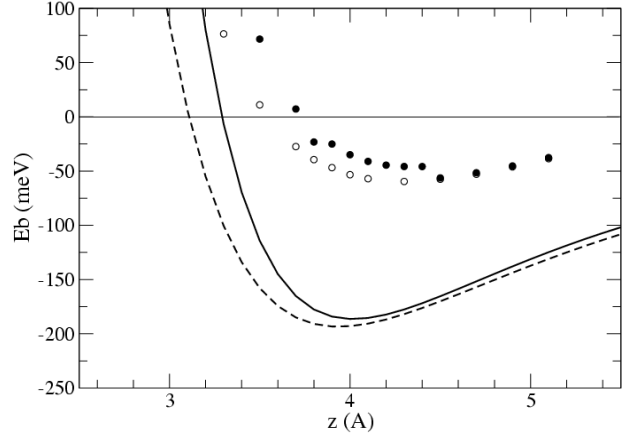


FIG. 2: Binding energy of Xe on Pb(111) in the *top* and *hollow* configuration using pure PW91 (full and empty circles, respectively) and DFT/vdW-WF (solid and dashed line, respectively), as a function of the distance z from the surface.

the *hollow* and *bridge* configurations for Ne and Kr on Pb(111), we qualitatively confirm the trend observed by Zhang *et al.*,¹⁶ being our estimated activation energies (1.3 meV for Ne and 6.0 meV for Kr) of the same order of magnitude as those reported in ref. 16 (0.7 meV for Ne and 2.5 meV for Kr). However, such small energy values are comparable to (or even smaller than) the expected accuracy of the computed binding energies, thus making quantitative estimates of the hopping probabilities¹⁶ (which depend exponentially on the aforementioned activation energies) rather questionable.

IV. CONCLUSIONS

In summary, by analyzing the results of our study of the adsorption of RG atoms on the Cu(111) and Pb(111) surfaces, one can conclude that the inclusion of the vdW corrections by the DFT/vdW-WF method systematically improves upon the estimates for the binding energies as obtained by a standard GGA approach. In particular, using a pure PW91 functional the binding is underestimated in all cases, while equilibrium distances are overestimated. For all the system considered the vdW correction term represents the dominant part of the binding energy, although, particularly for RG adsorption on Pb(111), the pure PW91 approach gives a substantial contribution. However, vdW interactions appear not to play a critical role in the adsorption site preference (the same result has been obtained by Zhang *et al.*¹⁶ studying the interaction of Ne and Kr on Pb(111)): Xe on Cu(111) clearly prefers the *top* site, while for Ne, Ar, and Kr on Cu(111) the differences in binding energies relative to different adsorption sites are so small that is not

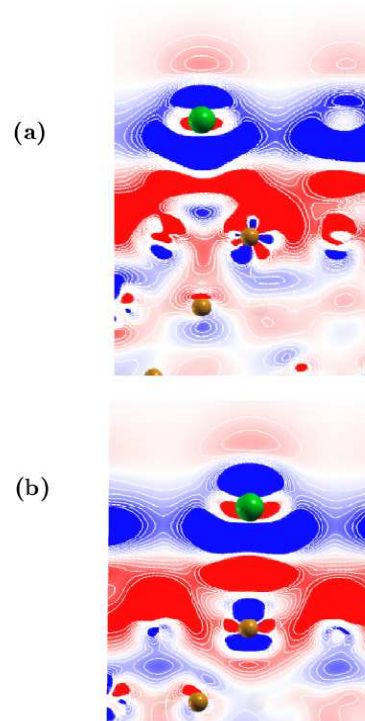


FIG. 3: Electron density difference of Xe on Cu(111) in (a) *hollow* and (b) *top* site shown in a plane perpendicular to the surface, within the range of $\pm 1 \times 10^{-4} e/\text{bohr}^3$. Red (light grey) and blue (dark grey) represent electron accumulation and depletion, respectively. The green and orange spheres indicate the Xe and Cu atoms, respectively.

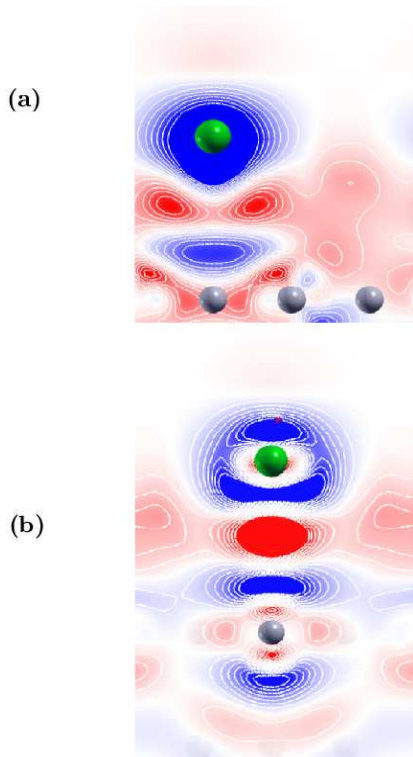


FIG. 4: Electron density difference of Xe on Pb(111) in (a) *hollow* and (b) *top* site shown in a plane perpendicular to the surface, within the range of $\pm 1 \times 10^{-4} e/\text{bohr}^3$. Red (light grey) and blue (dark grey) represent electron accumulation and depletion, respectively. The green and grey spheres indicate the Xe and Pb atoms, respectively.

easy to attribute a definitive preference; instead, the *hollow* configuration tends to be preferred for adsorption of all the considered RGs on Pb(111), in agreement with previous calculations and experimental observations.^{15,16} Moreover, the Pb(111) substrate is subject, upon rare-gas adsorption, to a significantly smaller change in the work function, and to a correspondingly smaller (in absolute value) induced dipole moment, than Cu(111). Given these relevant peculiarities of the Pb(111) surface, where the *hollow* site is undoubtedly favored for adsorption of RG atoms, this surface would represent an ideal substrate to study, both theoretically and experimentally, high-coordination adsorption sites.

V. ACKNOWLEDGEMENTS

We thank very much F. Costanzo and F. Toigo for useful discussions.

-
- * Present Address: Center for Chemistry, IHTM, University of Belgrade, Njegoševa 12, 11001, Belgrade, Serbia, and Scuola Normale Superiore, piazza dei Cavalieri 7, I-56126 Pisa, Italy.
- ² L. W. Bruch, M. W. Cole, and E. Zaremba, *Physical Adsorption: Forces and Phenomena* (Clarendon Press, Oxford, 1997).
 - ³ G. Vidali, G. Ihm, H. Y. Kim, M. W. Cole, *Surf. Sci. Rep.* **12**, 133 (1991).
 - ⁴ J. M. Gottlieb, *Phys. Rev. B* **42**, 5377 (1990).
 - ⁵ Th. Seyller, M. Caragiu, R. D. Diehl, P. Kaukasoina, M. Lindroos, *Chem. Phys. Lett.* **291**, 567 (1998); M. Caragiu, Th. Seyller, R. D. Diehl, *Phys. Rev. B* **66**, 195411 (2002).
 - ⁶ B. Narloch, D. Menzel, *Chem. Phys. Lett.* **290**, 163 (1997).
 - ⁷ R. D. Diehl, Th. Seyller, M. Caragiu, G. S. Leatherman, N. Ferralis, K. Pussi, P. Kaukasoina, M. Lindroos, *J. Phys.: Condens. Matter* **16**, S2839 (2004).
 - ⁸ J. L. F. Da Silva, C. Stampfl, M. Scheffler, *Phys. Rev. Lett.* **90**, 066104 (2003).
 - ⁹ J. L. F. Da Silva, C. Stampfl, M. Scheffler, *Phys. Rev. B* **72**, 075424 (2005).
 - ¹⁰ J. L. F. Da Silva, C. Stampfl, *Phys. Rev. B* **77**, 045401 (2008).
 - ¹¹ A. E. Betancourt, D. M. Bird, *J. Phys.: Condens. Matter* **12**, 7077 (2000).
 - ¹² P. Lazic, Z. Crljen, R. Brako, B. Gumhalter, *Phys. Rev. B* **72**, 245407 (2005).
 - ¹³ M. C. Righi, M. Ferrario, *J. Phys.: Condens. Matter* **19**, 305008 (2007).
 - ¹⁴ X. Sun, Y. Yamauchi, *J. Appl. Phys.* **110**, 103701 (2011).
 - ¹⁵ N. Ferralis, H. I. Li, K. J. Hanna, J. Stevens, H. Shin, F. M. Pan, R. D. Diehl, *J. Phys.: Condens. Matter* **19**, 056011 (2007).
 - ¹⁶ Y. N. Zhang, F. Hanke, V. Bortolani, M. Persson, R. Q. Wu, *Phys. Rev. Lett.* **106**, 236103 (2011).
 - ¹⁷ L. Bruschi, M. Pierno, G. Fois, F. Ancilotto, G. Mistura, C. Boragno, F. Buatier de Mongeot, U. Valbusa, *Phys. Rev. B* **81**, 115419 (2010).
 - ¹⁸ P. S. Bagus, V. Staemmler, C. Wöll, *Phys. Rev. Lett.* **89**, 096104 (2002).
 - ¹⁹ See, for instance, W. Kohn, Y. Meir, D. E. Makarov, *Phys. Rev. Lett.* **80**, 4153 (1998).
 - ²⁰ R. Eisenhitz, F. London, *Z. Phys.* **60**, 491 (1930).
 - ²¹ K. E. Riley, M. Pitoňák, P. Jurečka, P. Hobza, *Chem. Rev.* **110**, 5023 (2010).
 - ²² P. L. Silvestrelli, *Phys. Rev. Lett.* **100**, 053002 (2008).
 - ²³ P. L. Silvestrelli, K. Benyahia, S. Grubisić, F. Ancilotto, F. Toigo, *J. Chem. Phys.* **130**, 074702 (2009).
 - ²⁴ P. L. Silvestrelli, *J. Phys. Chem. A* **113**, 5224 (2009).
 - ²⁵ Y. Andersson, D. C. Langreth, B. I. Lundqvist, *Phys. Rev.*

- Let. **76**, 102 (1996).
- ²⁶ N. Marzari, D. Vanderbilt, Phys. Rev. B **56**, 12847 (1997).
- ²⁷ P. L. Silvestrelli, Chem. Phys. Lett. **475**, 285 (2009).
- ²⁸ P. L. Silvestrelli, F. Toigo, F. Ancilotto, J. Phys. Chem. C **113**, 17124 (2009).
- ²⁹ A. Ambrosetti, P.L. Silvestrelli, J. Phys. Chem. C **115**, 3695 (2011).
- ³⁰ S. Baroni *et al.*, www.quantum-espresso.org .
- ³¹ WanT code by A. Ferretti *et al.*, www.wannier-transport.org .
- ³² E. Abad, Y. J. Dappe, J. I. Martnez, F. Flores, J. Ortega, J. Chem. Phys. **134**, 044701 (2011).
- ³³ J. P. Perdew, Y. Wang, Phys. Rev. B **45**, 13244 (1992).
- ³⁴ J. P. Perdew, K. Burke, M. Ernzerhof, Phys. Rev. Lett. **77**, 3865 (1996).
- ³⁵ R. R. Rehr, E. Zaremba, W. Kohn, Phys. Rev. B **12**, 2062 (1975); J. Tao, J. P. Perdew, A. Ruzsinszky, Phys. Rev. B **81**, 233102 (2010).
- ³⁶ K. Lee, Y. Morikawa, D. C. Langreth, Phys. Rev. B **82**, 155461 (2010).
- ³⁷ M. Dion, H. Rydberg, E. Schröder, D. C. Langreth, B. I. Lundqvist, Phys. Rev. Lett. **92**, 246401 (2004); G. Roman-Perez, J. M. Soler, Phys. Rev. Lett. **103**, 096102 (2009).
- ³⁸ M. Vanin, J. J. Mortensen, A. K. Kelkkanen, J. M. Garcia-Lastra, K. S. Thygesen, K. W. Jacobsen, Phys. Rev. B **81**, 081408 (2010).
- ³⁹ E. Cheng, M. W. Cole, W. F. Saam, J. Treiner, Phys. Rev. B **48**, 18214 (1993).
- ⁴⁰ T. Thonhauser, V. R. Cooper, S. Li, A. Puzder, P. Hyldgaard, D. C. Langreth, Phys. Rev. B **76**, 125112 (2007).
- ⁴¹ C. J. Fall, N. Binggeli, A. Baldereschi, J. Phys.: Condens. Matter **11**, 2689 (1999).
- ⁴² C. J. Fall, N. Binggeli, A. Baldereschi, Phys. Rev. B **61**, 8489 (2000).
- ⁴³ B. Sun, P. Zhang, Z. Wang, S. Duan, X.-G. Zhao, X. Ma, Q.-K. Xue, Phys. Rev. B **78**, 035421 (2008).
- ⁴⁴ L. D. Schmidt, R. Gomer, J. Chem. Phys. **45**, 1605 (1966).
- ⁴⁵ P. Zeppenfeld, *Physics of Covered Solid Surfaces*, Börnstein, New Series, Group III, Vol. 42: Numerical data and functional relationships in science and technology, Subvol. A: Adsorbed layers on surfaces (Springer-Verlag, Berlin, 2001), p. 67.

TABLE I: Binding energy, E_b in meV, of RG atoms on the Cu(111) surface computed using the standard DFT-PW91 calculation, and including the vdW corrections using our DFT/vdW-WF method, compared to the LDA result, the vdW-DF method by Langreth *et al.*³⁷ and available theoretical and experimental (in parenthesis) reference data.

system	PW91	DFT/vdW-WF	LDA	vdW-DF	ref.
Ne-Cu(111) <i>hollow</i>	-17.6	-31.6	-55.7	-56.1	—
Ne-Cu(111) <i>top</i>	-17.5	-31.1	-55.4	-55.9	—
Ne-Cu(111) <i>bridge</i>	-17.6	-31.0	-55.3	-56.1	—
Ar-Cu(111) <i>hollow</i>	-13.0	-67.8	-88.9	-106.6	—
Ar-Cu(111) <i>top</i>	-13.0	-71.9	-94.5	-106.3	-85 ^a
Ar-Cu(111) <i>bridge</i>	-13.0	-70.6	-89.4	-106.4	—
Kr-Cu(111) <i>hollow</i>	-20.3	-134.2	-117.6	-135.7	—
Kr-Cu(111) <i>top</i>	-20.3	-131.1	-126.0	-135.8	-119 ^a
Kr-Cu(111) <i>bridge</i>	-20.3	-130.0	-118.4	-135.7	—
Xe-Cu(111) <i>hollow</i>	-22.9	-194.5	-199.3	-167.4	-276 ^b , -268 ^c
Xe-Cu(111) <i>top</i>	-23.1	-208.1	-221.9	-167.7	-280 ^b , -183 ^a , -277 ^c (-190 ^c)
Xe-Cu(111) <i>bridge</i>	-17.1	-191.2	-201.0	-167.4	-278 ^b

^aref.3.

^bref.12.

^cref.8.

TABLE II: Binding energy, E_b in meV, of RG atoms on the Pb(111) surface computed using the standard DFT-PW91 calculation, and including the vdW corrections using our DFT/vdW-WF method, compared to the LDA result, the vdW-DF method by Langreth *et al.*³⁷ and available theoretical and experimental (in parenthesis) reference data.

system	PW91	DFT/vdW-WF	LDA	vdW-DF	ref.
Ne-Pb(111) <i>hollow</i>	-31.2	-59.8	-49.4	-71.4	-51.6 ^a
Ne-Pb(111) <i>top</i>	-27.8	-49.1	-42.9	-63.3	-46.8 ^a
Ne-Pb(111) <i>bridge</i>	-19.8	-58.5	-49.1	-64.6	—
Ar-Pb(111) <i>hollow</i>	-23.5	-82.4	-78.3	-100.8	—
Ar-Pb(111) <i>top</i>	-22.1	-75.0	-64.2	-95.3	—
Ar-Pb(111) <i>bridge</i>	-22.7	-84.5	-76.6	-100.1	—
Kr-Pb(111) <i>hollow</i>	-30.8	-132.8	-98.8	-136.9	-134.9 ^a
Kr-Pb(111) <i>top</i>	-29.1	-109.8	-81.6	-130.9	-125.1 ^a
Kr-Pb(111) <i>bridge</i>	-24.0	-126.8	-96.7	-136.1	—
Xe-Pb(111) <i>hollow</i>	-59.6	-193.5	-142.0	-192.2	-172.6 ^a
Xe-Pb(111) <i>top</i>	-56.3	-186.4	-116.1	-186.4	—
Xe-Pb(111) <i>bridge</i>	-52.7	-188.9	-138.6	-191.2	—

^aref.16.

^bref.15.

TABLE III: Adsorption energy (E_a , see text for the definition), in meV, of Xe atoms on the Cu(111) and Pb(111) surfaces computed using the standard DFT-PW91 calculation, and including the vdW corrections using our DFT/vdW-WF method, compared to the LDA result, the vdW-DF method by Langreth *et al.*³⁷ and available experimental (in parenthesis) reference data.

system	PW91	DFT/vdW-WF	LDA	vdW-DF	ref.
Xe-Cu(111) <i>hollow</i>	-51.4	-289.3	-297.3	-268.9	—
Xe-Cu(111) <i>top</i>	-51.6	-302.9	-319.9	-269.2	(-227 ^a)
Xe-Cu(111) <i>bridge</i>	-45.6	-286.0	-299.0	-268.9	—
Xe-Pb(111) <i>hollow</i>	-62.5	-205.5	-147.9	-252.2	(-191 ^a)
Xe-Pb(111) <i>top</i>	-59.2	-198.4	-122.0	-246.4	—
Xe-Pb(111) <i>bridge</i>	-55.6	-200.9	-146.9	-251.2	—

^aref.15.

TABLE IV: Equilibrium RG adatom-surface distance, in Å, on the Cu(111) surface computed using the standard DFT-PW91 calculation, and including the vdW corrections using our DFT/vdW-WF method, compared to the LDA result, the vdW-DF method by Langreth *et al.*³⁷ and available theoretical and experimental (in parenthesis) reference data; the sum, s , of the vdW radii of the RG atom and the Cu atom is also reported.

system	PW91	DFT/vdW-WF	LDA	vdW-DF	ref.	s
Ne-Cu(111) <i>hollow</i>	3.90	3.59	3.10	3.70	—	2.94
Ne-Cu(111) <i>top</i>	3.90	3.57	3.09	3.68	—	2.94
Ne-Cu(111) <i>bridge</i>	3.90	3.60	3.10	3.68	—	2.94
Ar-Cu(111) <i>hollow</i>	4.50	3.48	3.19	3.90	—	3.28
Ar-Cu(111) <i>top</i>	4.50	3.45	3.15	3.86	3.53 ^a	3.28
Ar-Cu(111) <i>bridge</i>	4.50	3.43	3.19	3.86	—	3.28
Kr-Cu(111) <i>hollow</i>	4.50	3.32	3.21	3.99	—	3.42
Kr-Cu(111) <i>top</i>	4.50	3.36	3.17	3.99	—	3.42
Kr-Cu(111) <i>bridge</i>	4.50	3.35	3.20	3.99	—	3.42
Xe-Cu(111) <i>hollow</i>	4.70	3.42	3.00	4.10	3.40 ^b , 3.31 ^c	3.56
Xe-Cu(111) <i>top</i>	4.40	3.36	2.90	4.09	3.45 ^b , 3.2 ^d , 3.25 ^c (3.60 ^e)	3.56
Xe-Cu(111) <i>bridge</i>	4.70	3.41	3.00	4.10	—	3.56

^aref.3.

^bref.14.

^cref.8.

^dref.12.

^eref.5.

TABLE V: Equilibrium RG adatom-surface distance, in Å, on the Pb(111) surface computed using the standard DFT-PW91 calculation, and including the vdW corrections using our DFT/vdW-WF method, compared to the LDA result, the vdW-DF method by Langreth *et al.*³⁷ compared to the LDA result, and available theoretical and available theoretical and experimental (in parenthesis) reference data; the sum, s , of the vdW radii of the RG atom and the Pb atom is also reported.

system	PW91	DFT/vdW-WF	LDA	vdW-DF	ref.	s
Ne-Pb(111) <i>hollow</i>	3.80	3.41	3.10	3.70	3.5 ^a	3.56
Ne-Pb(111) <i>top</i>	4.00	3.68	3.40	3.90	3.8 ^a	3.56
Ne-Pb(111) <i>bridge</i>	3.80	3.36	3.27	3.50	—	3.56
Ar-Pb(111) <i>hollow</i>	4.40	3.68	3.40	4.00	—	3.90
Ar-Pb(111) <i>top</i>	4.40	4.04	3.60	4.22	—	3.90
Ar-Pb(111) <i>bridge</i>	4.50	3.77	3.43	4.10	—	3.90
Kr-Pb(111) <i>hollow</i>	4.40	3.69	3.40	4.14	3.8 ^a	4.04
Kr-Pb(111) <i>top</i>	4.40	3.98	3.70	4.24	3.9 ^a	4.04
Kr-Pb(111) <i>bridge</i>	4.30	3.79	3.51	4.13	—	4.04
Xe-Pb(111) <i>hollow</i>	4.30	3.93	3.50	4.30	(3.95 ^b)	4.18
Xe-Pb(111) <i>top</i>	4.50	4.02	3.70	4.30	—	4.18
Xe-Pb(111) <i>bridge</i>	4.70	3.93	3.55	4.31	—	4.18

^aref.16.

^bref.15.

TABLE VI: Work-function change, in eV, and induced dipole moment (in parenthesis), in debyes, for RGs adatoms on the Cu(111) and Pb(111) surfaces, at equilibrium geometries.

system	<i>hollow</i>	<i>top</i>
Ne-Cu(111)	-0.04 (-0.02)	-0.03 (-0.01)
Ar-Cu(111)	-0.28 (-0.13)	-0.37 (-0.17)
Kr-Cu(111)	-0.54 (-0.24)	-0.37 (-0.17)
Xe-Cu(111)	-0.53 (-0.24)	-0.57 (-0.26)
Ne-Pb(111)	-0.03 (-0.03)	-0.03 (-0.03)
Ar-Pb(111)	-0.10 (-0.08)	-0.03 (-0.03)
Kr-Pb(111)	-0.11 (-0.09)	-0.05 (-0.04)
Xe-Pb(111)	-0.13 (-0.11)	-0.04 (-0.03)